Int. J. Electrochem. Sci., 15 **(2020)** 12395 – 12409, doi: 10.20964/2020.12.28

International Journal of
ELECTROCHEMICAL
SCIENCE
www.electrochemsci.org

Study on Pt(Sn)/TiO_2-C as Anodic Catalysts for Direct Ethanol Fuel Cell

Chiu-Hung Liu[1], *Mao-Huang Liu*[2,*], *Ying-Huei Liu*[3], *Chia-Jung Lu*[4], *Chia-Chih Chang*[5], *Chih-Chia Wang*[3,6] *and Chen-Bin Wang*[3,6,*]

[1] Graduate School of National Defense Science, Chung Cheng Institute of Technology, National Defense University, Taoyuan, Taiwan, ROC
[2] Department of Chemistry, Fu-Jen Catholic University, New Taipei City, Taiwan, ROC
[3] Department of Chemical and Materials Engineering, Chung Cheng Institute of Technology, National Defense University, Taoyuan, Taiwan, ROC
[4] Department of Chemistry, National Taiwan Normal University, Taipei, Taiwan, ROC
[5] Department of Applied Chemistry, National Chiao Tung University, Hsinchu, Taiwan, ROC
[6] System Engineering and Technology Program, National Chiao Tung University, Hsinchu, Taiwan, ROC
[*]E-mail: 061355@mail.fju.edu.tw and chenbinwang@gmail.com

Received: 31 July 2020 / *Accepted:* 25 September 2020 / *Published:* 31 October 2020

This research concentrated on the use of a modified Pt/C anodic catalyst with titania (TiO_2) and tin (Sn) to enhance the utilization and efficiency of a direct ethanol fuel cell. The TiO_2-doped active carbon support (TiO_2-C) was prepared by the impregnation method. Then, using platinum chloride ($PtCl_4$) and tin (II) chloride dihydrate ($SnCl_2 \cdot 2H_2O$) as precursors, a Pt(Sn)/TiO_2-C anodic catalyst was fabricated by the formic acid reduction method. Further, a series of Pt(Sn)/TiO_2-C anodic catalysts were coated on carbon paper as working electrodes. Performance evaluations were executed by cyclic voltammetry (CV) and chronoamperometry for the ethanol electro-oxidation, and CO stripping voltammetry was performed in an acid solution at room temperature. Characterization of the series Pt(Sn)/TiO_2-C catalysts displayed that all catalysts revealed uniform dispersion of platinum with a diameter around 3 - 6 nm and a high electrochemically active surface area. Apparently, the doping of TiO_2 and Sn could disperse the active species, and lower the potential of the ethanol electro-oxidation to improve the ethanol oxidation reaction (EOR). In addition, the inclusion of TiO_2 and Sn could promote CO stripping by the surface active OH_{ad} sites and through the formation of a $PtSn_2$ alloy at a lower oxidizing potential.

Keywords: Pt(Sn)/TiO_2-C anodic catalyst; Electro-oxidation; Cyclic voltammetry.

1. INTRODUCTION

In the past decades, the development of direct alcohol fuel cells (DAFCs) has been extensive and made them a possible power source. These power sources are based on proton exchange membrane fuel cells and use alcohol as fuel for portable electric devices such as mobile phones, charger, notebooks, and electric vehicles [1-14]. They can be directly converted into hydrogen for power generation through a reformer. Compared to other fuel cells, DAFCs only demand a short time from startup to stable power generation, coupled with high stability, low fuel composition risk, low operating temperature, and convenient fuel replenishment. Among the alcohols, methanol (MeOH) [1-3, 11, 12], ethanol (EtOH) [4-6, 9-11, 13, 14] and ethylene glycol (EG) [7, 8, 10, 11] are popular energy resources owing to their high energy density and easy access. Ethanol is an active ingredient in alcoholic beverages, while both methanol and ethylene glycol refer to toxic alcohols that can result in severe metabolic acidosis [15]. In this study, ethanol was locked and the goal of the research was to investigate how to design the electrocatalyst in order to improve the capability of the complete electro-oxidation of ethanol.

In general, highly dispersed active species on high surface area carbon-based electrocatalysts are potentially adopted for ethanol oxidation while enhance the C–C breaking bond. Among these, noble metals (Pt, Pd, Rh, Au) with unique catalytic activities are commonly chosen [1-14, 16-23]. Titanium dioxide (TiO_2) possesses a high activity and catalytic stability in acidic solutions [19, 24, 25]. Javier et al. [24] used TiO_2/SBA-15 as a photocatalyst to execute the oxidation of alcohol under UV irradiation. Brian et al. [25] confirmed the performance of a Pt/TiO_2 catalyst when applied to the electro-oxidation of ethanol. Reaction intermediate of CO easily poisoned platinum to become inactive of electro-oxidation for anodic catalysts. In order to inhibit the poisoning of anodic catalysts, Simoes et al. [26] revealed that Sn-Pt bimetallic catalysts can mitigate the poisoning effect of CO on ethanol electro-oxidation.

Based on the approaches, a comparative study on series Pt(Sn)/TiO_2-C anodic catalysts fabricated by the formic acid reduction method was studied in this work, and the efficiency of the electro-oxidation of ethanol and CO stripping were evaluated using cyclic voltammetry (CV).

2. EXPERIMENTAL

The supports of the TiO_2-doped (10, 20, 30 and 40 wt%) active carbon (S.A. 240 $m^2 \cdot g^{-1}$, Cabot) were prepared by the impregnation method (assigned as 10, 20, 30 and 40TiO_2-C). The appropriate mass active carbon was added into a 250 mL flask and mixed with a suitable proportion of 2-propanol-$Ti(OC_4H_9)_4$-HNO_3 for 24 h stirring at room temperature, after which the suspension was filtered and washed with distilled water. The obtained precipitate was dried overnight at 110 °C. Series Pt(Sn)/C and Pt(Sn)/TiO_2-C anodic catalysts were fabricated by the formic acid reduction method [27] using platinum chloride ($PtCl_4$) and tin dichloride dihydrate ($SnCl_2 \cdot 2H_2O$) as precursors. An appropriate mass of support powder (C or TiO_2-C) was suspended in a formic acid solution, and then precursor salt solutions of $PtCl_4$ (Strem Chemicals) and/or $SnCl_2 \cdot 2H_2O$ (Acros Organics) were slowly added to the suspension of support for 6 h stirring at 60 °C in water bath. The blend was then cooled to room temperature, filtered and washed with distilled water until the washing solution approached pH 7. Further, the precipitate was dried overnight at 110 °C. Both the Pt and Sn loadings were controlled at

10 wt%, separately.

A JEM-2010 (JEOL) transmission electron microscope (TEM) was used to observe the distribution and average size of the series anodic catalysts under an acceleration voltage of 200 kV. X-ray diffraction (XRD) characterization was executed using a MAC Science MXP18 X-ray diffractometer and Cu K_α as a source. The 2θ angle was explored in the range of 20° and 80° with a scan rate of $6°\cdot min^{-1}$ (with 0.02° steps). In each temperature programmed reduction (TPR) survey, a fresh 50 mg sample was added to the U-shaped cell, and then the TPR temperature was increased from – 50 to 200 °C at a rate of $7\ °C\cdot min^{-1}$. The reduction was carried out through a flow of 10% H_2 in N_2. The surface area of the catalysts was measured through the BET equation by nitrogen physisorption.

The electrochemical measurement was executed in a three-electrode cell using an electrochemical analyzer (CH Instruments 611C) at 25 °C. Painting series Pt(Sn)/TiO_2-C anodic catalyst on carbon paper were used as the working electrode. The loading of the anodic catalyst on the central region of the carbon paper was $4\ mg\cdot cm^{-2}$. Both reference and counter electrodes were chosen the saturated calomel electrode (SCE) and Pt foil. All electrode potentials referred to SCE in the electrochemical measurements. The cyclic voltammogramcyclic voltammetry (CV) test of the ethanol oxidation reaction (EOR) was conducted between – 0.2 to 1.0 V potential vs SCE. The scan rate in the 0.5 M H_2SO_4 and 1 M ethanol solutions was $10\ mV\cdot s^{-1}$. The electrolyte solution was purged under nitrogen gas before each experiment. An evaluation of the hydrogen adsorption and desorption area (– 0.15 to 0.25 V) on the CV in a 0.5 M H_2SO_4 solution at 25 °C with a scan rate of $50\ mV\cdot s^{-1}$ was employed to obtain the electrochemical active surface (EAS) of Pt according to equation (1) [28].

$$EAS = Q_H/M_{Pt}\cdot Q_{Href} \qquad (1)$$

Q_H is the average charge of the electro-adsorption and desorption of hydrogen atoms on the Pt surface, M_{Pt} is the mass of the loaded Pt, and Q_{Href} is the charge required to oxidize the monolayer of H_2 on the Pt surface (assuming $0.21\ mC\cdot cm^{-2}$ corresponds to the surface density of 1.3×10^{15} $atom\cdot cm^{-2}$) [29, 30]. Measurement of the chronoamperometry was carried out at 0.45 V with scanning a scanning time of 3600 s in an ethanol solution. The CO stripping was executed using voltammetry. In the working electrode compartment, flow through 0.1% CO in Ar solution at a rate of $140\ ml\cdot min^{-1}$ for 30 min adsorption, and set the scan rate to $10\ mV\cdot s^{-1}$ in the range of – 0.2 to 1.0 V in 0.5 M H_2SO_4 solution.

3. RESULTS AND DISCUSSION

The XRD patterns of a series of Pt/TiO_2-C and PtSn/TiO_2-C anodic catalysts are displayed in Figure 1. No distinct TiO_2 diffraction peaks were discovered in the XRD patterns of Pt/TiO_2-C and PtSn/TiO_2-C. It was indicated that the manufactured TiO_2-modified support was amorphous. The Pt/TiO_2-C catalysts (Fig. 1(a)) showed dispersion of the platinum particles (d_{Pt} ~ 5 - 6 nm), and the PtSn/TiO_2-C catalysts (Fig. 1(b)) showed a single well-defined and well-dispersed $PtSn_2$ alloy (d_{Pt} ~ 3 - 4 nm). The diffraction peaks near 39.8°, 46.3° and 68° were ascribed to the (111), (200) and (220) refractive index planes of Pt with a face-centered cubic (fcc) structure, whereas the broad peaks at 24° (111), 39° (220) and 46° (311) revealed the presence of a $PtSn_2$ phase as reported previously [31-34].

In addition, the diffraction peaks (39° and 46°) were slightly turned to a lower angle regarding to the Pt, further demonstration Pt and Sn atoms form a solid solution.

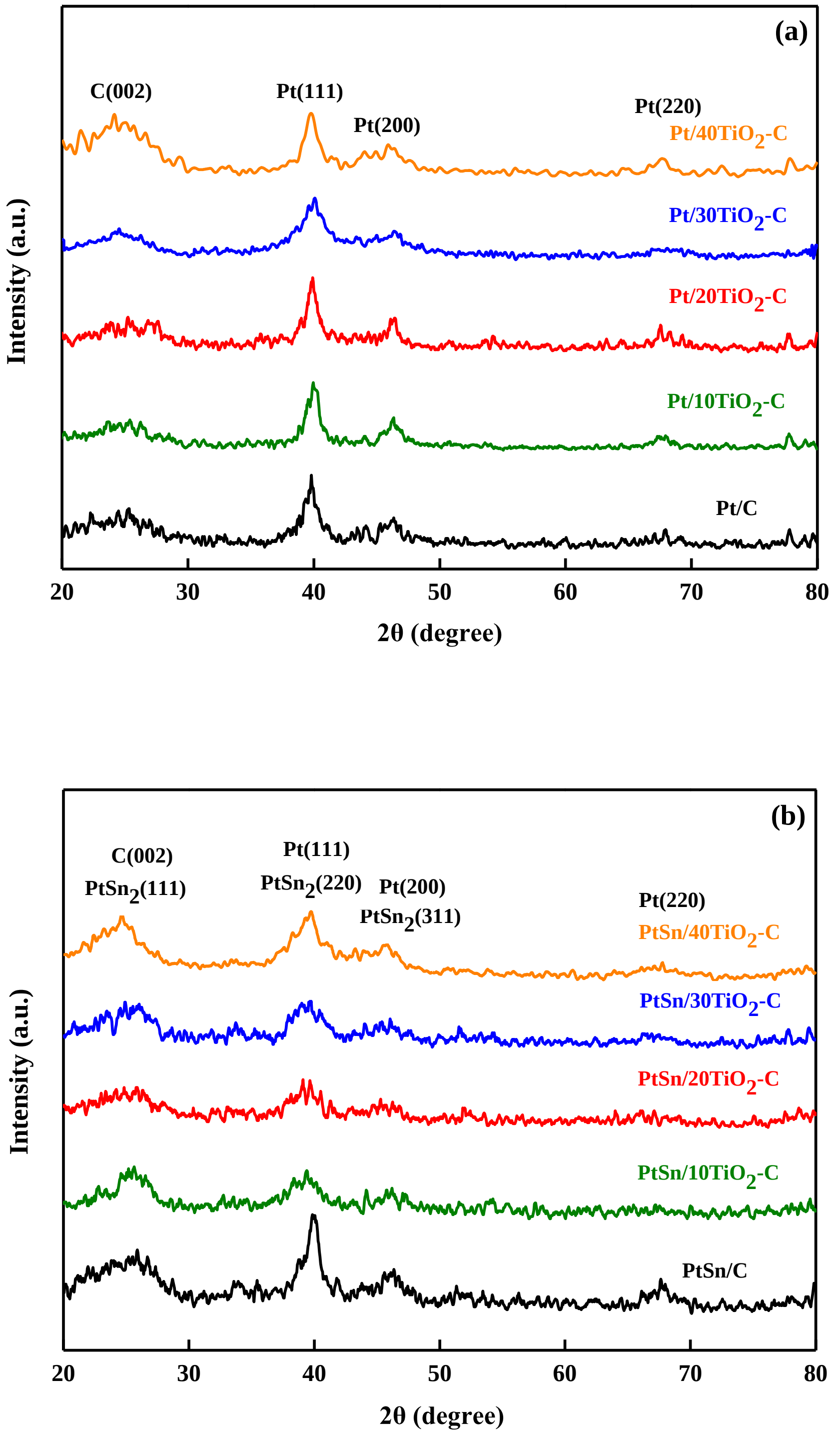

Figure 1. XRD patterns of (a) Pt/TiO_2-C (b) PtSn/TiO_2-C anodic catalysts.

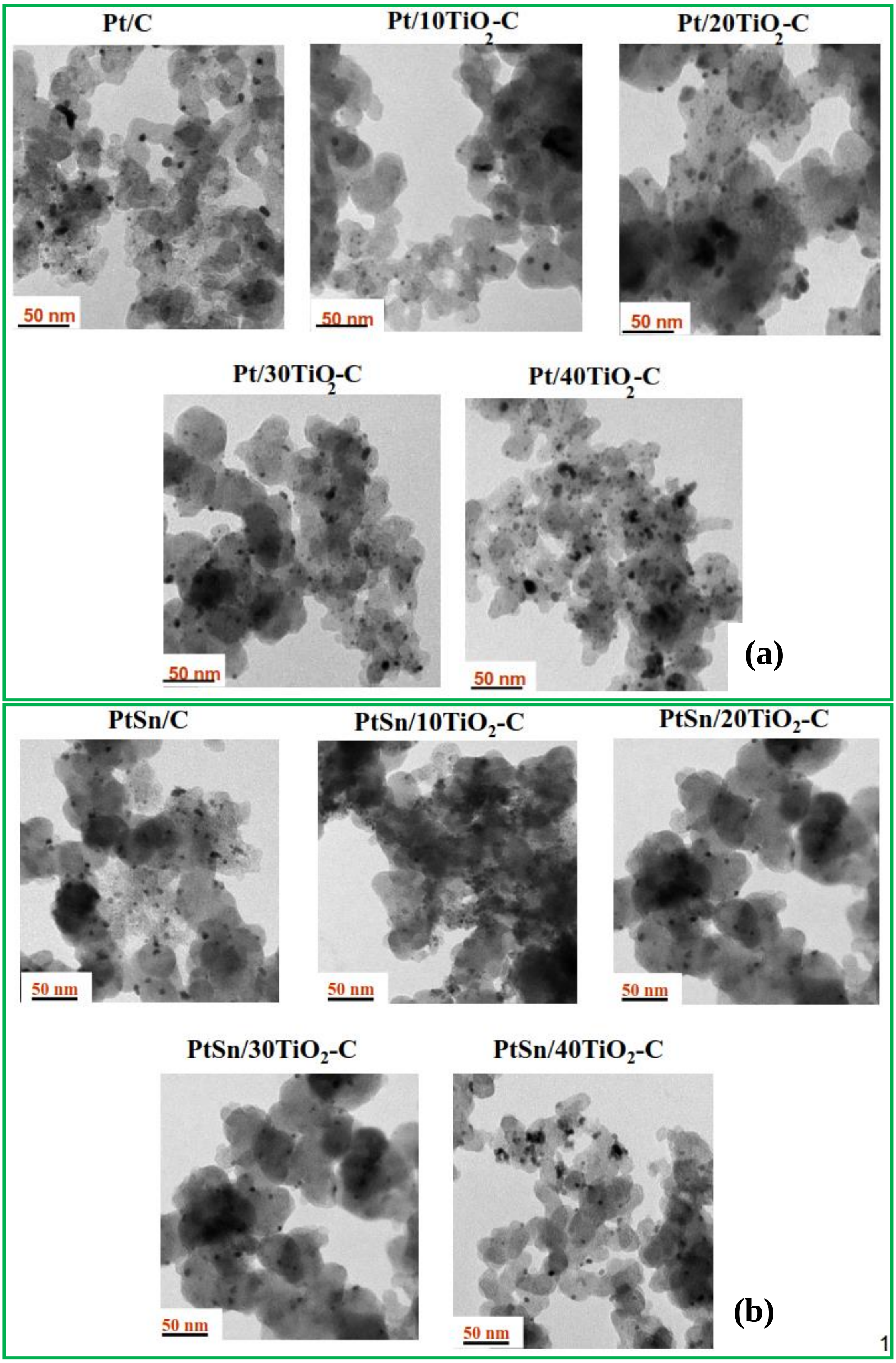

Figure 2. TEM images of (a) Pt/TiO_2-C (b) PtSn/TiO_2-C anodic catalysts.

In the performance of TiO_2 as a supported noble metal for the catalytic oxidation of HCHO, Zhang et al. [35] indicated that Pt particles on TiO_2 are well dispersed. A comparison of the diffraction patterns of platinum found broadening of the peaks and contraction of the 2θ on the Pt/TiO_2-C and PtSn/TiO_2-C catalysts. These results indicated that the modification of active carbon with TiO_2 could disperse the active species and that the addition of tin could incorporate into the fcc lattice of Pt to form a well-dispersed alloy. To estimate the particle size of the platinum, the Pt (111) and $PtSn_2$ (220) diffraction peaks were selected to calculate the particle size according to the Scherrer formula, as listed in Table 1. Simultaneously, TEM micrographs of both series Pt/TiO_2-C and PtSn/TiO_2-C catalysts are indicated in Figure 2. The observed mean nanoparticle size was about 5 ~ 6 nm for Pt/TiO_2-C (Fig. 2(a)) and 3 ~ 4 nm for the PtSn/TiO_2-C catalysts (Fig. 2(b)), as listed in Table 1, which was matched to the calculated values from XRD.

Table 1. Physical and chemical characterization of series Pt(Sn)/TiO_2-C anodic catalysts.

Catalyst	d (nm)*		Surface area (m^2/g)	TPR (°C)	
	XRD*	TEM		T_{r1}	T_{r2}
Pt/C	6.0	6.9	196	-10	---
Pt/10TiO_2-C	5.7	5.8	194	-11	121
Pt/20TiO_2-C	5.5	5.0	184	-16	117
Pt/30TiO_2-C	5.2	4.8	181	-20	97
Pt/40TiO_2-C	5.3	4.9	178	-16	100
PtSn/C	5.5	5.6	221	-24	152
PtSn/10TiO_2-C	3.7	3.9	210	-27	135
PtSn/20TiO_2-C	3.6	3.7	193	-31	133
PtSn/30TiO_2-C	3.4	3.1	189	-35	139
PtSn/40TiO_2-C	3.7	3.9	179	-34	134

*: Calculated from the XRD, the Pt (111) and $PtSn_2$ (220) diffraction peaks are selected to calculate the particle size by Scherrer formula.

The TPR profiles of both the series Pt/TiO_2-C and PtSn/TiO_2-C anodic catalysts are indicated in Figure 3. Both reduction signals (listed in Table 1) could be distinguished according to previous literature [36, 37]. The signal at the low temperature (T_{r1}: - 45 ~ - 5 °C) was attributed to the reduction of Pt^sO_x and/or $PtSn_2{}^sO_x$ (Pt^s and $PtSn_2{}^s$ are the surface species of Pt metal and $PtSn_2$ alloy) in weak interaction with the support as following equations.

$Pt^sO_x + x\ H_2 \rightarrow Pt^s + x\ H_2O$ (2)

$PtSn_2{}^sO_x + x\ H_2 \rightarrow PtSn_2{}^s + x\ H_2O$ (3)

The signal at the high temperature (T_{r2}: 95 ~ 125 °C) came from the strong interaction of Pt and/or $PtSn_2$ with support. A comparison of these anodic catalysts found that the temperature of the highly dispersed $PtSn_2{}^sO_x$ was lower than that of the Pt^sO_x. Also, the modification of active carbon with TiO_2 could well-dispersed active species to lower the reduction temperature of the catalyst.

The EAS of different anodic catalysts can be measured by cyclic voltammograms (CVs) under an acidic electrolyte, which can be measured according to the average charge of hydrogen electro-adsorption and desorption on the Pt surface. Figure 4 shows the CVs of both the series Pt/TiO_2-C and PtSn/TiO_2-C anodic catalysts in a 0.5 M H_2SO_4 solution at 25 °C, and the calculated EAS is listed in Table 2. It could provide quantitative information about the relative number of active sites on the surface to understand the electro-catalytic activity among series anodic electrodes. Based on the quantitative calculation of the current densities in the double-layer zone reduction, the EAS of the series PtSn/TiO_2-C catalysts were 1.2 times higher than those of the series Pt/TiO_2-C catalysts and were six times higher than that of the Pt/C catalyst. This feature could be attributed to the characteristics of bimetallic catalysts containing oxygen-philic transition metals, namely Ti, Mo, Os, Ru and Sn [38, 39], for accelerating the hydrolysis of water to provide more surface hydroxyl species (OH_{ad}).

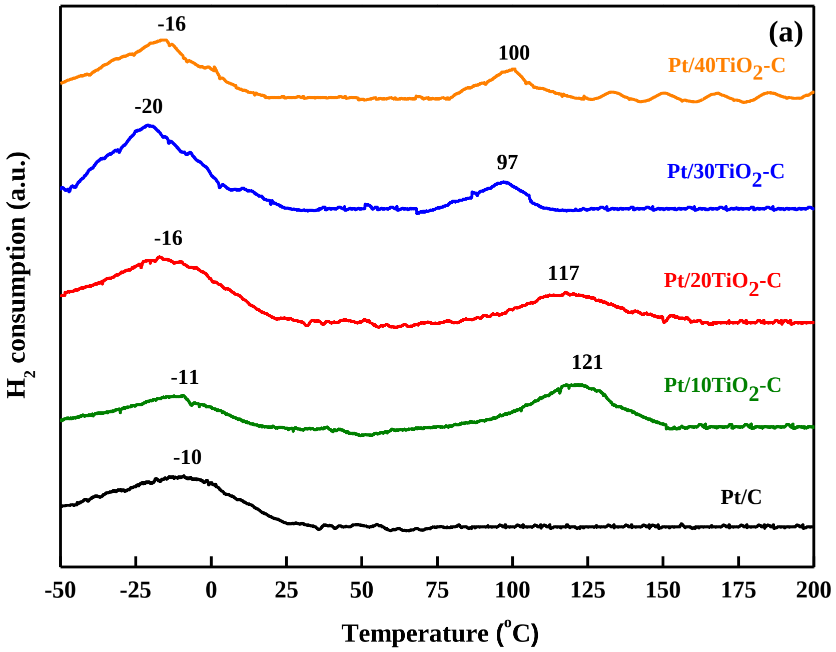

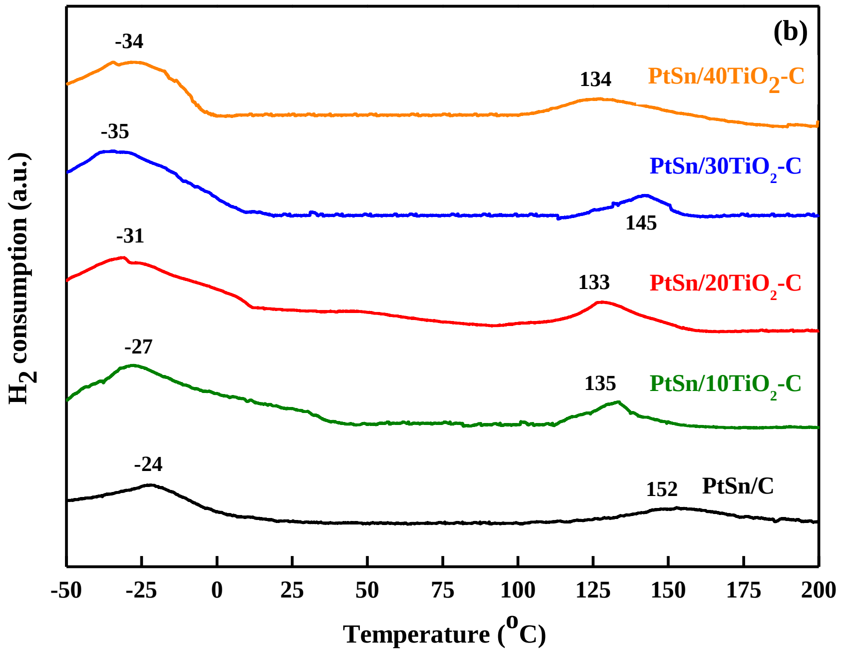

Figure 3. TPR profiles of (a) Pt/TiO$_2$-C (b) PtSn/TiO$_2$-C anodic catalysts.

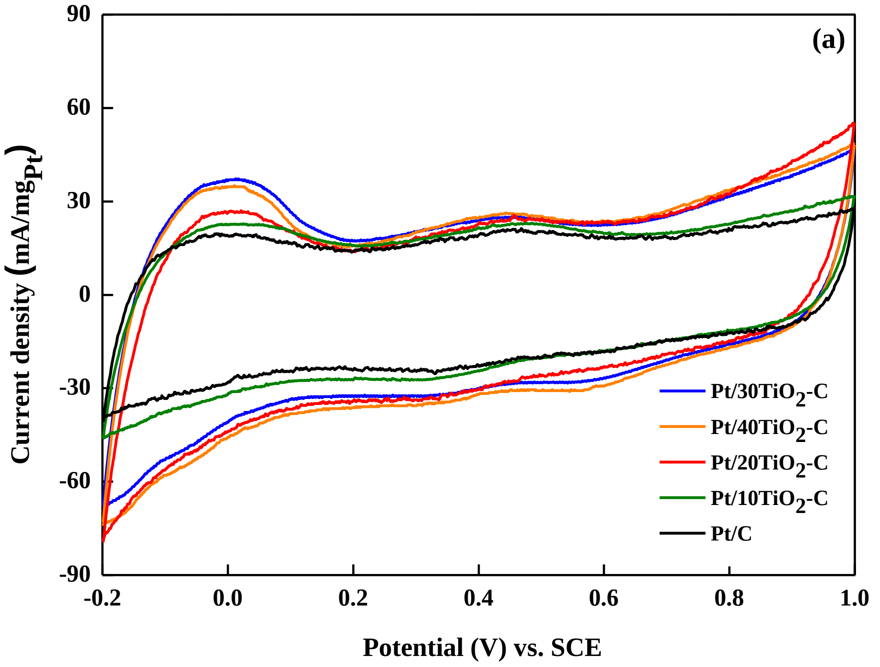

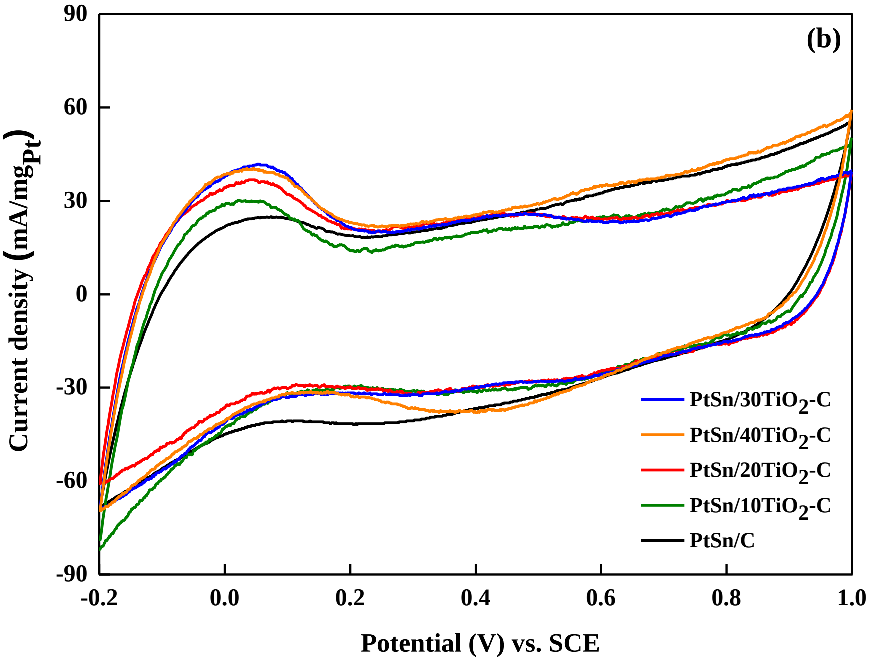

Figure 4. CVs of the (a) Pt/TiO_2-C (b) PtSn/TiO_2-C electrodes in 0.5 M H_2SO_4 solution with a scan rate of 50 mV·s^{-1} at 25 °C.

The results demonstrated that both the addition of TiO_2 and Sn could improve the true surface area of Pt. It was deduced that modification of the Pt/C anodic catalyst with the addition of TiO_2 and Sn could enhance the dispersal of active species. Therefore, it could be expected that the tendency of activity for the ethanol electro-oxidation was: PtSn/TiO_2-C > Pt/TiO_2-C > PtSn/C > Pt/C. These results also demonstrated that the EAS varied significantly with the TiO_2 loading within the Pt(Sn)/TiO_2-C catalysts. A higher loading of TiO_2 would cause encapsulation of the surface Pt and decrease the surface active site, meanwhile, the 30 wt% TiO_2 exhibited the highest EAS and “intrinsic” activities among the series catalysts.

The as-prepared Pt/TiO_2-C and PtSn/TiO_2-C anodic catalysts were assessed to determine the catalytic activity of EOR. For the purpose of comprehending the roles of Sn and TiO_2, a comparative test of the Pt/C catalyst under the same conditions was also carried out. Figure 5 displays the forward sweep of the CVs of both the series Pt/TiO_2-C and PtSn/TiO_2-C anodic catalysts in a 0.5 M H_2SO_4 + 1 M C_2H_5OH electrolyte. A scan rate of 10 mV·s^{-1} at 30 °C was used to assess the oxidation of ethanol in the potential between – 0.2 to 1.0 V vs SCE. Based on the maximum peak current during the forward scan (I_P, listed in Table 2), the trend for the performance of EOR was PtSn/TiO_2-C > Pt/TiO_2-C > PtSn/C > Pt/C, which was consistent with the measurement of EAS. Compared with the Pt/C and PtSn/C catalysts, the EOR current densities of Pt/TiO_2-C and PtSn/TiO_2-C were significantly increased by a factor of two with the loading of TiO_2, revealing that the EOR kinetics for the PtSn/TiO_2-C and Pt/TiO_2-C catalysts were faster. Compared with the dispersed platinum particles, it was apparent that the doping of TiO_2 and Sn could disperse the active species and favor the removal of adsorbed intermediates with the surface active OH_{ad} sites, and then further the oxidation of the adsorbed intermediate species.

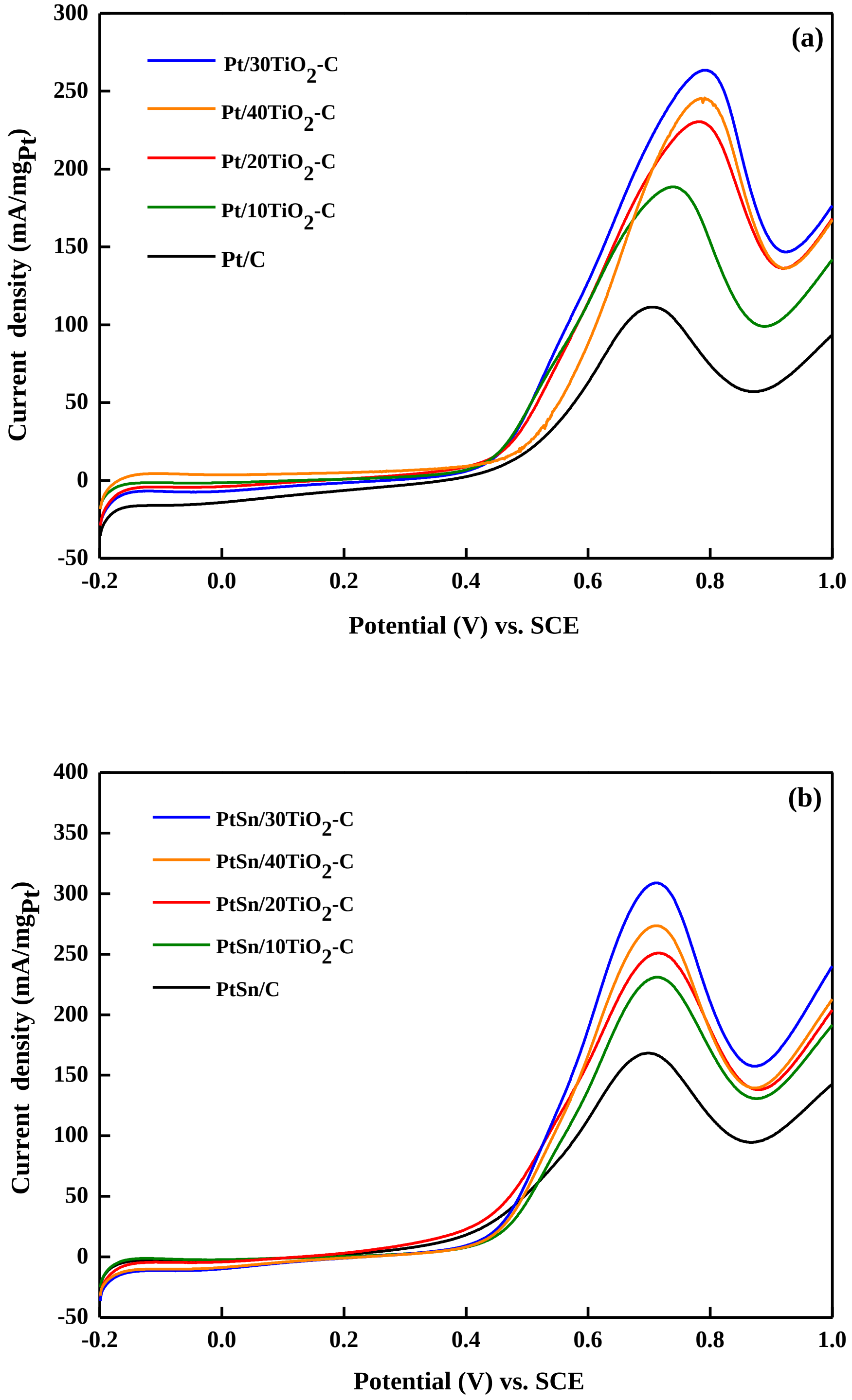

Figure 5. Cyclic voltammograms of the (a) Pt/TiO_2-C (b) $PtSn/TiO_2$-C electrodes in 1 M ethanol/0.5 M H_2SO_4 solution with a scan rate of 50 $mV \cdot s^{-1}$ at 25 °C.

A comparison of the electro-oxidation peak of ethanol on Pt/C and PtSn/C with Xin et al. [31]

found that the E_p are about 0.15 V and 0.08 V higher than our fabricated anodic catalysts. Considering that TiO_2/Pt/C and Pt/C with Qiu et al. [40], the E_p are about 0.1 V and 0.12 V higher than our fabricated anodic catalysts. Therefore, both TiO_2 and Sn could reduce the potential of ethanol electro-oxidation, thereby increasing EOR. Accordingly, the series PtSn/TiO_2-C represented a more suitable electrocatalyst, as it had better catalytic activity than the Pt/C and PtSn/C catalysts during ethanol electro-oxidation. The optimal loading of TiO_2 could guard against the agglomeration or deformation of the catalyst during ethanol oxidation. Among the series anodic catalysts, PtSn/30TiO_2-C showed a higher dispersion of active species, reducibility and electrochemical active surface, thereby exhibiting the best catalytic performance.

Table 2. Performance of series Pt(Sn)/TiO_2-C electrodes in terms of EAS, EOR and CO stripping.

Catalyst	EOR		EAS (cm^2/mg_{Pt})	CO electro-oxidation	
	I_p (mA/mg_{Pt})*	E_p (V)**		E_{onset} (V)#	E_{CO} (V)##
Pt/C	111	0.70	49	0.52	0.63
Pt/10TiO_2-C	189	0.74	152	0.41	0.56
Pt/20TiO_2-C	230	0.78	179	0.42	0.55
Pt/30TiO_2-C	263	0.79	264	0.38	0.54
Pt/40TiO_2-C	245	0.79	229	0.40	0.55
PtSn/C	168	0.70	99	0.38	0.55
PtSn/10TiO_2-C	231	0.71	215	0.38	0.42
PtSn/20TiO_2-C	251	0.72	244	0.24	0.42
PtSn/30TiO_2-C	310	0.71	317	0.25	0.43
PtSn/40TiO_2-C	274	0.71	275	0.25	0.43

*: Maximum peak current **: Maximum peak potential in EOR #: Onset potential ##: Maximum peak potential in CO stripping

In order to appraise the electrochemical stability of ethanol electro-oxidation in an acidic media, further chronoamperometric measurements were performed to evaluate the EOR durability. The selected PtSn/30TiO_2-C, Pt/30TiO_2-C and Pt/C anodic catalysts were maintained at 0.45 V and scanned for 3600 s in a 0.5 M H_2SO_4 + 1 M C_2H_5OH electrolyte. The amperometric *I-t* curves are displayed in Figure 6. These three catalysts revealed a fast decay of current density within the first few minutes and then maintained a stable current density. The current density decay was attributed to the surface being blocked by the CO_{ad} intermediate species, and the decaying rate depended on the strength of the adsorbed CO [41]. The Pt/C catalysts modified with TiO_2 and Sn provided more surface active OH_{ad} sites to strip the CO_{ad} species, and they maintained as higher current density. Among these, the PtSn/30TiO_2-C catalyst indicated less degradation and higher current density compared to the Pt/C and Pt/30TiO_2-C catalysts, which was consistent with the measured values of the CV curves. The EOR current density over the PtSn/30TiO_2-C catalyst for 3600 s approached 60 mA/mg_{Pt}, and the current density attained 30 mA/mg_{Pt} and 10 mA/mg_{Pt}, respectively for the Pt/30TiO_2-C and Pt/C catalysts. This result indicates that the PtSn/30TiO_2-C anodic catalyst had better stability and activity than the Pt/30TiO_2-C and Pt/C catalysts on the ethanol electro-oxidation.

Since CO_{ad} is the primary poisoning intermediate species in the electro-oxidation of ethanol, a favorable catalyst with excellent CO electro-oxidation capacity needed to be provided, which could be confirmed by the detection of CO stripping. The curves of the CO stripping for the selected PtSn/30TiO_2-C, Pt/30TiO_2-C and Pt/C anodic catalysts are displayed on Figure 7. The onset potentials (E_{onset}, as listed in Table 2) and peak potentials (E_{CO}, as listed in Table 2) of the CO oxidation were 0.25 and 0.43 V for PtSn/30TiO_2-C, 0.38 and 0.54 V for Pt/30TiO_2-C, 0.52 and 0.63 V for Pt/C, respectively. Previous literatures [38, 39, 42] have revealed that modification of the Pt catalyst with Sn and TiO_2 can generate numerous accessible OH_{ad} sites, which enhances in removing the CO_{ad} on the Pt sites by further transferring the CO_{ad} into CO_2.

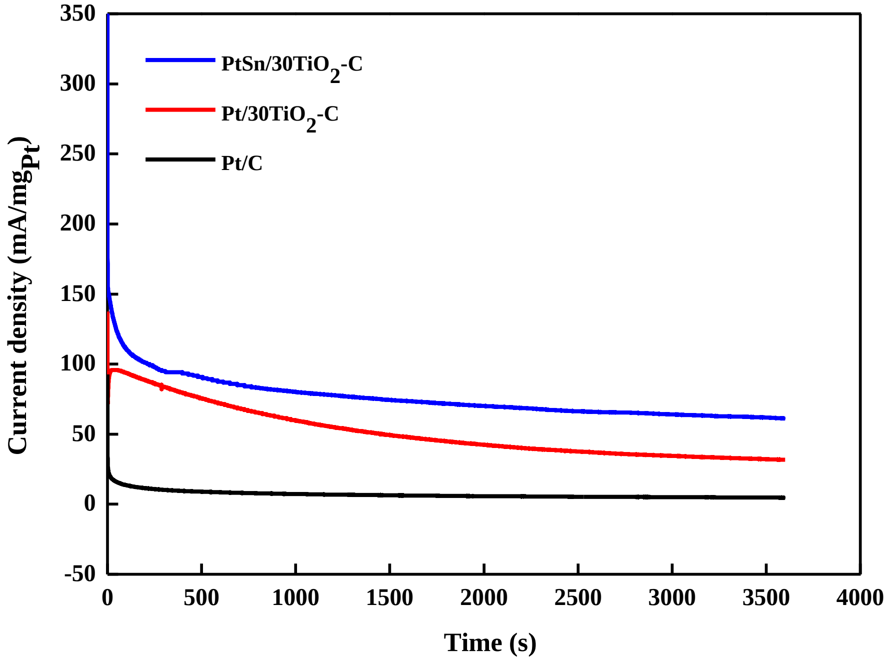

Figure 6. Current density-time curves at 0.45 V for scanning 3600 s for the selected Pt/C, Pt/30TiO_2-C and PtSn/30TiO_2-C electrodes in ethanol solution.

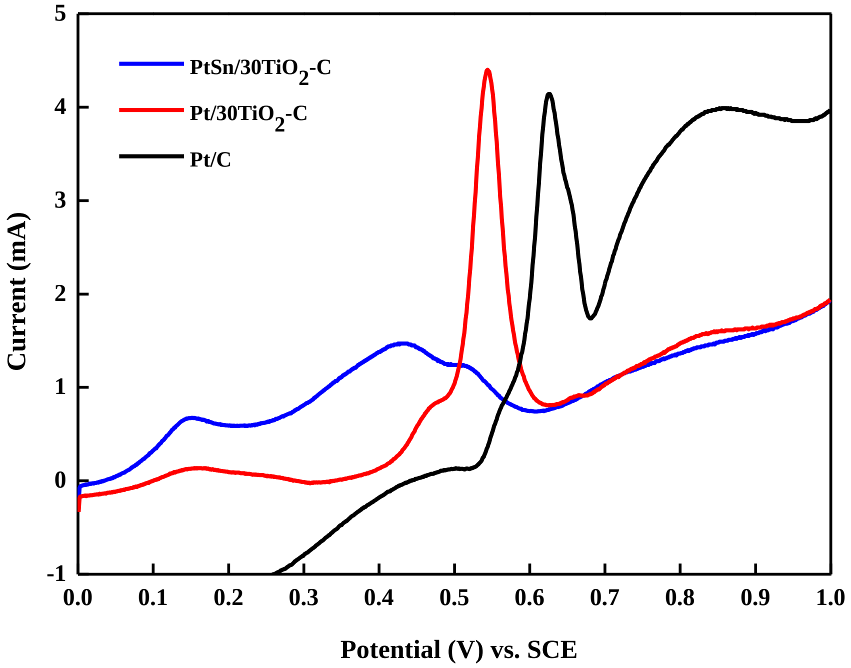

Figure 7. Cyclic voltammograms for CO stripping of selected Pt/C, Pt/30TiO_2-C and PtSn/30TiO_2-C electrodes (adsorption time 30 min, sweep rate 50 mV·s^{-1}).

We supposed that the reaction of TiO_2 with water would product the Ti-OH functional groups, and Sn with Pt form $PtSn_2$ alloy, they can effectively reduce the oxidation of CO to CO_2 oxidation potential. A comparison of the CO stripping on TiO_2/Pt/C with Qiu et al. [40] found that the E_{onset} and E_{CO} are about 0.21 V and 0.11 V higher than our fabricated PtSn/30TiO_2-C catalyst. This result implied that the addition of TiO_2 and Sn could promote the ability to oxidize CO to CO_2 at a lower potential, which could help increase the number of active sites and promote the electro-oxidation of ethanol.

4. CONCLUSIONS

The results of this study demonstrated that the addition of TiO_2 and Sn to an anodic catalyst will significantly affect the activity of ethanol electro-oxidation. Modification of the Pt/C anodic catalyst with TiO_2 and Sn can get well-dispersed and higher EAS of active species, which enhanced the electro-catalytic activity and lowered the potential. The addition of TiO_2 promoted CO stripping by the surface active OH_{ad} sites to reduce the CO oxidizing potential. Also, the formation of a $PtSn_2$ alloy enhanced the CO stripping at a lower oxidizing potential. Among the prepared series Pt(Sn)/TiO_2-C anodic catalysts, the PtSn/30TiO_2-C catalyst exhibited the best catalytic performance and stability, making it a possible candidate for application in direct alcohol fuel cells in the near further.

ACKNOWLEDGEMENT

We are pleased to acknowledge the financial support for this study from the Ministry of Science and Technology of the Republic of China under contract numbers of MOST 107-2113-M-606-001- and MOST 108-2113-M-606-001-.

References

1. A. Demirbas, *Progress in Energy and Combust. Sci.,* 33 (2007) 1.
2. L. Jiang, Z. Zhou, W. Li, W. Zhou, S. Song, H. Li, G. Sun, Q. Xin, *Energy and Fuels,* 18 (2004) 866.
3. C. Lamy, E.M. Belgsir, F. Hahn, C. Coutanceau, F. Vigier, *J. Appl. Electrochem.,* 563 (2004) 81.
4. S.C.S. Lai, S.E.F. Kleyn, V. Rosca, M.T.M. Koper, *J. Phys. Chem. C,* 112 (2008) 19080.
5. H. Wang, Z. Jusys, R.J. Behm, *J. Power Sources,* 154 (2006) 351.
6. R.L. Derek, L.G. Előd, *Electrochimica Acta,* 52 (2007) 4287.
7. H. Wang, Y. Zhao, Z. Jusys, R.J. Behm, *J. Power Sources,* 155 (2006) 33.
8. R.B. de Lima, V. Paganin, T. Iwasita, W. Vielstich, *Electrochimica Acta,* 49 (2003) 85.
9. L. Jiang, A. Hsu, D. Chu, R. Chen, *I. J. Hydrogen Energy,* 35 (2010) 365.
10. J.M. Sieben, M.M.E. Duarte, *I. J. Hydrogen Energy,* 36 (2011) 3313.
11. J.M. Sieben, M.M.E. Duarte, *I. J. Hydrogen Energy,* 37 (2012) 9941.
12. S. Sharma, B.G. Pollet, *J. Power Sources,* 208 (2012) 96.
13. L.A. Soares, C. Morais, T.W. Napporn, K.B. Kokoh, P. Olivi, *J. Power Sources,* 315 (2016) 47.
14. R.M.C. Silva, G.A. Camara, M.J. Giz, *Electrochimica Acta,* 308 (2019) 167.
15. J.A. Kraut, I. Kurtz, *Clinical Journal of the American Society of Nephrology,* 3 (2008) 208.
16. J. Bagchi, S.K. Bhattacharya, *J. Power Sources,* 163 (2007) 661.
17. Q. He, W. Chen, S. Mukerjee, S. Chen, F. Laufek, *J. Power Sources,* 187 (2009) 298.
18. C. Xu, L. Cheng, P. Shen, Y. Liu, *Electrochem. Comm.,* 9 (2007) 997.
19. J. Liu, J. Ye, C. Xu, S. Jiang, Y. Tong, *Electrochem. Comm.,* 9 (2007) 2334.
20. F.E. Teran, D.M. Santos, J. Ribeiro, K.B. Kokoh, *Thin Solid Films,* 520 (2012) 5846.
21. A.B. Delpeuch, F. Maillard, M. Chatenet, P. Soudant, C. Cremers, *Appl. Catal. B,* 181 (2016) 672.
22. A.B. Delpeuch, T. Asset, M. Chatenet, C. Cremers, *Fuel Cells,* 15 (2015) 352.
23. N. Erini, R. Loukrakpam, V. Petkov, E.A. Baranova, R. Yang, D. Teschner, Y. Huang, S.R. Brankovic, P. Strasser, *ACS Catal.,* 4 (2014) 1859.
24. M. Javier, H. Dirk, L.M. Marıa-Jose, S. Volker, B. Detlef, *Appl. Catal. B,* 62 (2006) 201.
25. E.H. Brian, V.M. Dzmitry, P. Derek, *Electrochem. Commun.,* 3 (2001) 395.
26. F.C. Simoes, D.M. dos Anjos, F. Vigier, J.M. Ĺeger, F. Hahna, C. Coutanceau, E.R. Gonzalez, G. Tremiliosi-Filho, A.R. de Andrade, P. Olivi, K.B. Kokoh, *J. Power Sources,* 167 (2007) 1.
27. C. Moitrayee, C. Abhik, G. Susanta, I. Basumallick, *Electrochimica Acta,* 54 (2009) 7299.
28. A. Pozio, M. De Francesco, A. Cemmi, F. Cardellini, L. Giorgi, *J. Power Sources,* 105 (2002) 13.
29. G. Faubert, D. Guay, J.P. Dodelet, *J. Electrochem. Soc.,* 145 (1998) 2985.
30. K. Woods, *J. Electrochem. Soc.,* 9 (1976) 1.
31. W. Zhou, Z. Zhou, S. Song, W. Li, G. Sun, P. Tsiakaras, Q. Xin, *Appl. Catal. B,* 46 (2003) 273.
32. J. Llorca, N. Homs, J.L.G. Fierro, J. Sales, P.R. de la Piscina, *J. Catal.,* 166 (1997) 44.
33. V. Grolier, R. Schmid-Fetzer, *J. Alloys Compd.,* 450 (2008) 264.
34. A.E. Alvarez, A.N. Gravina, J.M. Sieben, P.V. Messina, M.M.E. Duarte, *Mater. Sci. Eng. B,* 211 (2016) 26.
35. C.B. Zhang, H. He, K.I. Tanaka, *Appl. Catal. B,* 65 (2006) 37.
36. H. Armendáriz, A. Guzmán, J.A. Toledo, M.E. Llanos, A. Vázquez, G. Aguilar-Ríos, *Appl. Catal. A,* 211 (2001) 69.
37. A.D. Ballarini, S.R. de Miguel, A.A. Castro, O.A. Scelza, *Appl. Catal. A,* 467 (2013) 235.

38. E. Antolini, F. Colmati, E.R. Gonza´ lez, *Electrochem. Commun.,* 9 (2007) 398.
39. M. Barroso de Oliveira, L.P.R. Profeti, P. Olivi, *Electrochem. Commun.,* 7 (2005) 703.
40. H.Q. Song, X.P. Qiu, X.X. Li, F.S. Li, W.T. Zhu, L.Q. Chen, *J. Power Sources,* 170 (2007) 50.
41. X. He, C. Hu, *J. Power Sources*, 196 (2011) 3119.
42. J. Mann, N. Yao, Andrew B. Bocarsly, *Langmuir*, 22 (2006) 10432.